Flight Dynamics and Navigation Performance of the BioSentinel Mission

Andres Dono Perez[1]
Axient / NASA Ames Research Center, CA

Jose L. Alvarellos[2]
ASRC Federal/ NASA Ames Research Center, CA

Nahum Alem[2], Matthew Napoli[3]
NASA Ames Research Center, CA

Lisa Policastri[4], Ryan Lebois[4]
Space Exploration Engineering

BioSentinel was one of the ten 6U CubeSats launched by the Space Launch System (SLS) as part of the Artemis-I mission on November 16th, 2022. The spacecraft was deployed after the trans-lunar injection imparted by the upper stage of SLS, and performed a lunar flyby that provided the necessary energy to escape the Earth-Moon system into heliocentric space. The BioSentinel mission required flight dynamics support prior to flight to assess the deployment conditions and the trajectory design, as well as navigation support during flight, to provide orbit determination solutions for the mission and the Deep Space Network (DSN). This paper discusses the BioSentinel mission flight dynamics campaign, from mission design to the challenges and lessons learned encountered during flight.

I. Introduction

The BioSentinel spacecraft was launched on 16 November 2022 aboard the SLS Block 1 launch vehicle (LV) as part of the Artemis-I campaign (Refs. [1], [2]). The main purpose of this campaign was to place the Orion Multipurpose Crew Vehicle into a distant retrograde orbit (DRO) around the Moon (Refs. [3], [4]). In addition, ten 6U CubeSats ride-shared with Orion, and were placed in various azimuthal locations inside the Orion Stage Adapter (OSA), which connected the Orion capsule itself and SLS's upper stage, namely the Interim Cryogenic Propulsion System (ICPS). Originally 13 CubeSats were to ride along inside the OSA (Refs. [5], [6]). However, only ten, including BioSentinel, were aboard during the encapsulation phase in 2021.

Ia. Brief Overview of SLS, Orion and Rideshare CubeSat Deployments

The SLS launch took place from the Kennedy Space Center (KSC), launch pad 39B, and maximum dynamic pressure was achieved 70 seconds into the flight. The solid rocket boosters and then the first stage were discarded at approximately two, and a little over 8 minutes into the flight, respectively. The ICPS performed a Perigee Raising Maneuver (PRM), which started 51 minutes post-launch, and which thereafter also performed a TransLunar Injection (TLI) maneuver at 1:37 hours into the flight. Ten minutes after the TLI completion, ICPS/Orion separation took place via springs, and both the ICPS (with the OSA attached to it) and Orion were independently bound for lunar flyby.

[1] Flight Dynamics Lead, NASA Ames Research Center, Moffett Field, CA, 94035.
[2] Flight Dynamics Analyst, NASA Ames Research Center, Moffett Field, CA, 94035.
[3] BioSentinel project manager, NASA Ames Research Center, Moffett Field, CA, 94035.
[4] Flight Dynamics, Space Exploration Engineering.

Eighty-one seconds later, Orion performed a 1.7 m/s separation burn to further differentiate its trajectory with respect to the ICPS. An ICPS disposal burn, using its attitude control system thrusters, started approximately 30 minutes after separation, targeting depletion of its hydrazine load as well as a positive C3 energy. Finally, the various CubeSats were deployed from the ICPS/OSA at different deployment bus stops. Figure 1 shows the top-level sequence of events relevant for CubeSat deployments (Ref. [22]).

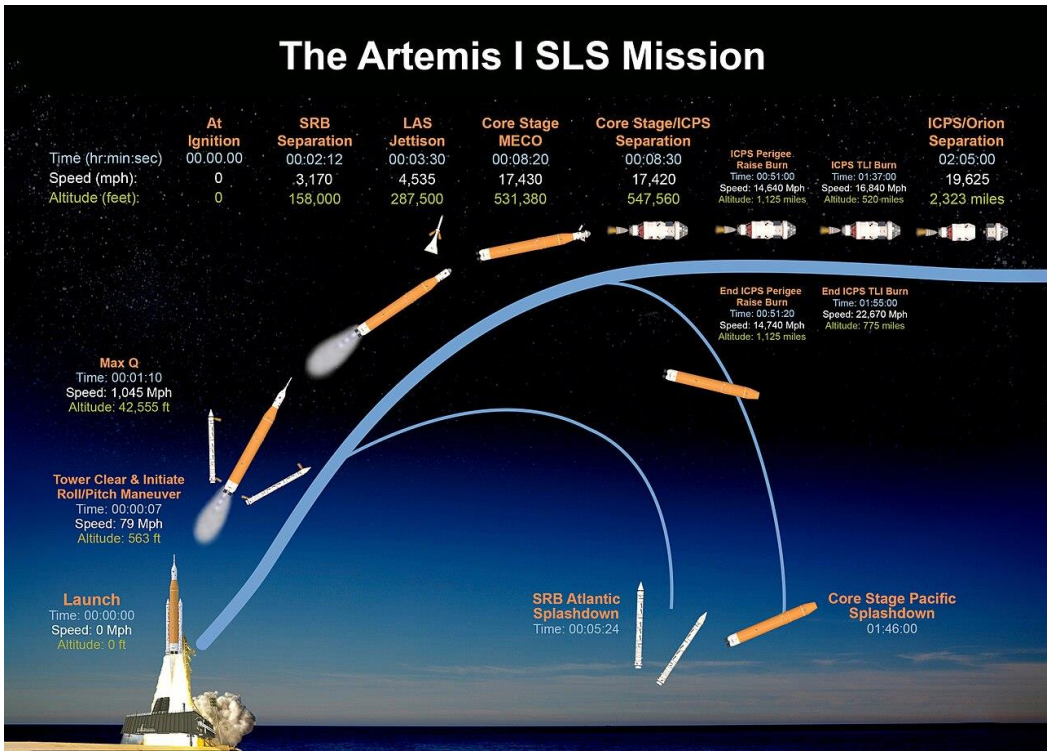

Figure 1. Main sequence of Events for the Artemis I mission relevant for the CubeSat deployments. The graph shows the timeline for a representative launch. The final sequence started with the SLS launch from KSC. The PRM maneuver was performed by the ICPS, approximately 51 minutes post-launch, and after the TLI maneuver was also performed by the ICPS. After this, ICPS and Orion were separated via springs, 02:05 hours into the flight, and both objects were then placed in independent lunar-bound trajectories. The various CubeSats were deployed from the ICPS/OSA and placed in lunar-bound trajectories after separation and the ICPS disposal burn. Image credits: National Space and Aeronautics Administration (NASA), Artemis-1 press release [22].

Detailed analyses based on dynamic Earth-Moon geometries, light conditions and SLS performance indicated that there were 10-16 launch opportunities per sidereal month, and the set of these opportunities was called an SLS Launch Period (Ref. [3]). Further, for any launch opportunity on a given day existed a launch window (LW) which was a span of time lasting from approximately 2 to 120 minutes, depending on mission constraints where launch could take place while meeting mission objectives. For example, Table 1 shows the launch windows for each day of Launch Period 28, which corresponded to the final launch on November 16th, 2022.

Table 1. Launch Windows for LP28, November 12th to 27th, 2022 (the conditions on the 20th and 21st of November 2022 did not comply with the launch requirements).

Launch Period (LP) Classification	Launch Window Opening				Launch Window		
	Date	Time	Zone	Lighting	Duration (mins)	Lit Duration (mins)	Lit (%)
LP28	11/12/2022	11:55:00 PM	EST	6.42 hours after sunset	24	0	0
LP28	11/14/2022	12:07:00 AM	EST	6.62 hours before sunrise	69	0	0
LP28	11/15/2022	12:20:00 AM	EST	6.42 hours before sunrise	112	0	0
LP28	11/16/2022	1:04:00 AM	EST	5.7 hours before sunrise	120	0	0
LP28	11/17/2022	1:04:00 AM	EST	5.71 hours before sunrise	120	0	0
LP28	11/18/2022	1:11:00 AM	EST	5.61 hours before sunrise	120	0	0
LP28	11/19/2022	1:45:00 AM	EST	5.05 hours before sunrise	120	0	0
LP28	11/20/2022	5:08:00 AM	EST	1.68 hours before sunrise	0	0	0
LP28	11/21/2022	6:14:00 AM	EST	0.6 hours before sunrise	0	0	0
LP28	11/22/2022	7:06:00 AM	EST	0.26 hours after sunrise	120	120	100
LP28	11/23/2022	7:34:00 AM	EST	0.71 hours after sunrise	120	120	100
LP28	11/24/2022	9:02:00 AM	EST	2.16 hours after sunrise	120	120	100
LP28	11/25/2022	10:10:00 AM	EST	3.28 hours after sunrise	111	111	100
LP28	11/26/2022	11:58:00 AM	EST	5.07 hours after sunrise	44	44	100
LP28	11/27/2022	12:34:00 PM	EST	4.86 hours before sunset	24	24	100

Ib. BioSentinel bus and payload

BioSentinel is an astrobiology small spacecraft mission. This project builds upon the extensive legacy at NASA Ames Research Center regarding CubeSats and space biology. Previous missions include PharmaSat, O/OREOS and GenSat-1 [7]. The payload, comprising 4U of the total 6U volume, consists of an experiment to measure DNA damage due to natural radiation in heliocentric space, far beyond the radiation-shielded LEO regime, on the standard organism *Saccharomyces cerevisiae* (budding yeast), of which there are two strains. The first is a wild type that is radiation tolerant, while the second is a mutant strain that is deficient in a gene that allows DNA repair following damage. The DNA damage is expected to be compared to (a) an identical sample aboard the ISS, as well as (b) another identical sample on the ground (Refs. [6], [8]). The two parts of the payload are a biosensor consisting of optical and microfluidics components (Refs. [9], [10]), and a Linear Energy Transfer (LET) spectrometer, built by NASA JSC RadWorks, whose purpose is to measure cosmic radiation including solar particle events such as coronal mass ejections (CMEs), and galactic cosmic radiation.

The Attitude Determination Control System (ADCS) includes one star tracker, one Inertial Measurement Unit (IMU), and five sun sensors. Three reaction wheels (RW) and six cold gas thrusters are the actuators that provide attitude control. The propulsion system is a cold-gas 3D-printed system with seven nozzles, and its two main components are a saturated vapor-liquid main tank, and a vapor-only plenum tank; the propellant is R-236fa, a commercially available hexafluorocarbon refrigerant [11]. Other bus components are the Electrical Power Systems (EPS), including the solar arrays (S/A) and batteries, and the low and medium-gain antennas. Figure 2 provides a detailed, exploded view of the spacecraft [12], and Figure 3 shows BioSentinel's body axes [11]. For communications, BioSentinel uses IRIS, an X-band transponder developed by JPL [12], which is a software defined radio. Telemetry, Tracking and Commanding (TT&C) is performed using the Deep Space Network (DSN; Ref. [13]), as well as the European Space Agency (ESA) antennas listed in Table 2.

Table 2. ESA Antennas utilized in the BioSentinel Mission.

Antenna Name	Country	Latitude	E. Longitude	Altitude (m)
Goonhilly	UK	+50°.0505	-5°.1836	108
New Norcia	Australia	-31°.0484	+116°.1930	252
Cebreros	Spain	+40°.4534	-4°.3684	794
Malargüe	Argentina	-35°.7764	-69°.3978	1,550

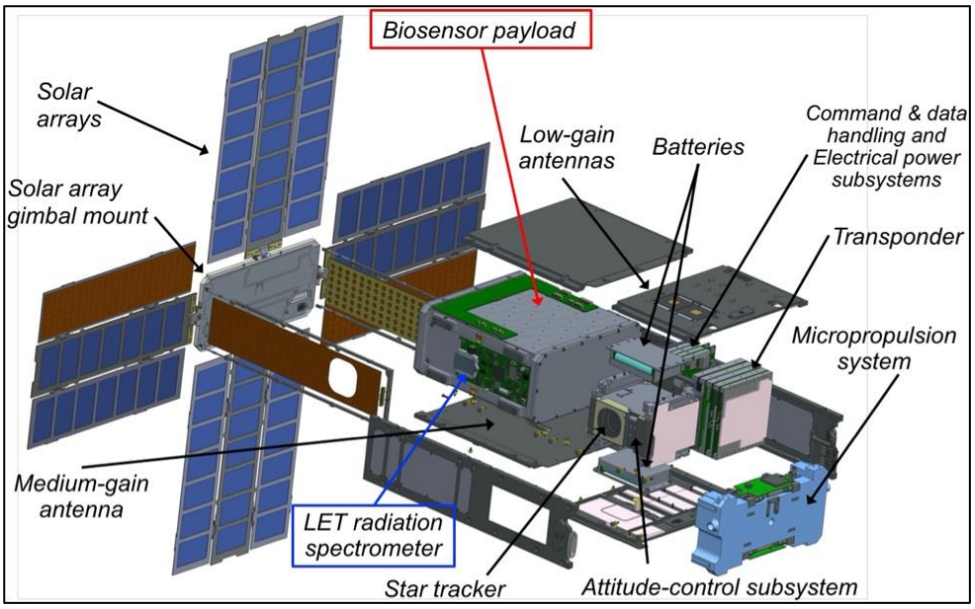

Figure 2. BioSentinel CubeSat, exploded view; from Ref. [12].

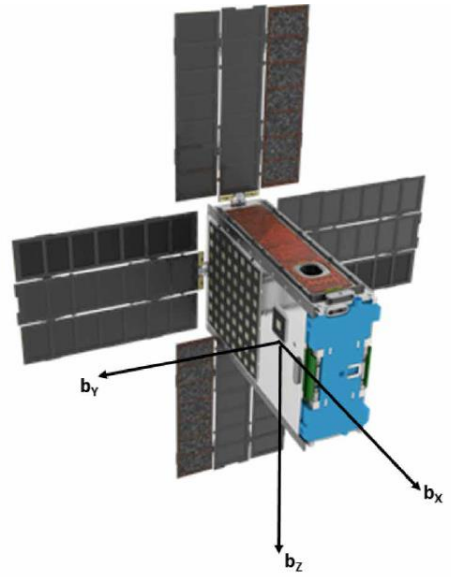

Figure 3. BioSentinel (shown with deployed solar arrays) body axes. The propulsion system is on the +X face, MGA and LGA patch antennas are on the +Y face (there are also LGA antennas on the -Y face, not shown), and the star tracker is shown on the -Z face. From Ref. [11].

II. Pre-Launch Activities

The BioSentinel Navigation Team pre-launch activities started years in advance. The first step consisted of analyzing the effects that the deployment from the ICPS could cause in a free flyer spacecraft on its way to a lunar flyby. Several launch dates and geometric conditions were proposed during the various years prior to launch. Therefore, the Navigation Team was adapting their analysis tools to satisfy the flight dynamics evolving requirements. In addition, Orbit Determination (OD) analysis was conducted to study the amount of tracking passes required to appropriately obtain ephemeris solutions that could bound the position and velocities uncertainties prior to the flyby. To achieve that, the team processed the tracking data through a filer and then a Smoother. These OD techniques sequentially step through the tracking data one point at a time, and then they filter the data in reverse to create a smoother solution. They also compute the state uncertainty in addition to other state information.

At the beginning of the mission, there is also a least-squares process needed to seed or start the filtering process, as an Initial-OD (IOD) process. Ansys's Orbit Determination Tool Kit (ODTK) version 7.0 was used to study orbital uncertainty evolution under various tracking assumptions, such as availability of ground stations and duration of passes. Other software tools the navigation team used are Ansys' Satellite Tool Kit (STK) version 12.4, as well as GMAT version 2020a. Thereafter, besides general familiarization with the Artemis I/SLS and BioSentinel missions [15], the main pre-launch activities for the navigation team were (i) production of predicted BioSentinel trajectories for various launch dates; (ii) Monte Carlo analyses; and (iii) mission rehearsals.

IIa. Predicted BioSentinel Trajectories

Once the Orion Multipurpose Crew Vehicle separated from the ICPS/OSA, the deployment of the CubeSats proceeded. Tyvak Nano-Satellite Systems Inc. produced the CubeSat dispensers that ride inside the ICPS/OSA and deploys each CubeSat in independent trajectories, a representation of this system is shown in Figure 4 (Refs. [15], [16]).

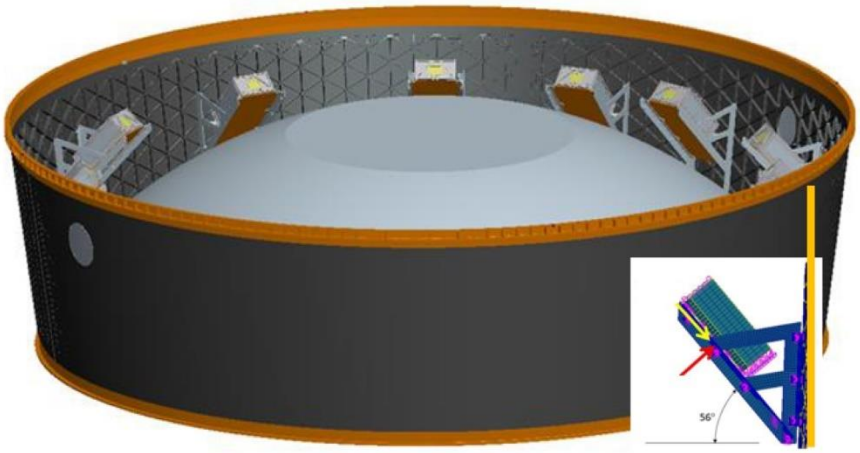

Figure 4. After the Orion capsule separation, the interior of the OSA (top part of ICPS) is exposed showing the CubeSat dispensers. The angle between the orange vertical line in the inset (which is aligned with both the ICPS's spin axis and velocity vector) and the OSA floor is 56 degrees. The structure was rotating at 1 rpm. Ref. [16].

For every day of a given LP, the navigation team from the NASA Marshall Space Flight Center (MSFC) provided the predicted state vector and attitude evolution of the ICPS, the starting epoch being the end of the ICPS disposal-burn. This information was provided for LW open circumstances; LW close; and instances in between for every minute of the LW that day (see Table 1). BioSentinel was the second CubeSat to deploy from the ICPS/OSA at Bus Stop One[3]. Each CubeSat's separation Epoch is a function of its azimuthal location inside the OSA (BioSentinel was located in Berth #5) and other parameters in the secondary spacecraft avionics unit [17], but for each proposed launch date the BioSentinel deployment was planned to take place just over two minutes after the ICPS disposal burn was complete.

The knowledge of the ICPS state vector and its spin axis orientation (the ICPS was rotating at 1 RPM), plus the expected deployment velocity, was a necessary but not sufficient information to compute BioSentinel's initial state vector. There was also the uncertainty in the ICPS spin at the exact moment of deployment, which translated into an unconstrained clock angle (0^o-360^o) at that deployment time. Therefore, to compute initial predictive ephemeris, the ICPS trajectory was propagated until BioSentinel's deployment epoch, when a random clock angle was selected to obtain the initial conditions. In turn this initial state vector is then propagated forward in time for several days past the lunar flyby, using an Earth-centered force model that considers:

- Earth's EMG08 gravity model (21x21 geopotential).
- Luni-solar point perturbations.

[3] For the first Bus Stop, the CubeSats were deployed in the following order: EQUULEUS (deployed at ICPS disposal burn end); BioSentinel; OMOTENASHI; and Lunar Ice Cube.

- Solar radiation pressure (SRP).

The SRP depends on the cross-sectional area to the Sun and the spacecraft mass. For BioSentinel, the maximum area is 0.316 m^2 when in spacecraft safe-mode, i.e., body -X axis pointing at the Sun and with all four solar panels deployed (see Fig. 3). This value periodically decreases somewhat during communication passes with ground stations, where the BioSentinel attitude is changed so that the patch antennas (on body axes +Y and -Y) point directly towards Earth. However, most of the time BioSentinel's cross-sectional area remains at its maximum value. BioSentinel's initial wet mass was 12.0 kg at launch time.

Predicted BioSentinel trajectories were computed for the opening and the closing for the various SLS launch windows (LWs had variable durations; see Table 1) within various LPs, therefore bracketing the possible orbital behavior of the CubeSat. Once BioSentinel deploys from the OSA, it is injected into a large, highly eccentric Earth-bound orbit. Table 3 shows a representative sample of the resulting BioSentinel separation orbits for three different launch dates. As computed from the listed semi-major axes, the orbital period of the separation orbit is approximately 10.3 days. BioSentinel deployment occurs at an altitude of approximately 41,200 km for each case, hence atmospheric drag was not a relevant perturbation for these simulations. Apogee is approximately 393,300 km, while the Moon's orbit has an average semi-major axis of 384,400 km. The reason the separation orbital elements are not identical at different launch dates is the fact that the ICPS/OSA (and therefore the CubeSats) are injected to go near the Moon. Since the Moon revolves around the Earth in a large orbit (approx. 1/4 of a Hill radius), it is highly perturbed by the Sun's gravity [18]. Therefore, different launch dates possibilities implied different separation orbits for BioSentinel.

Table 3. Representative sample of BioSentinel separation osculating orbital elements (J2000) for three different launch dates, assuming SLS LW-open circumstances. Epochs shown (UTC) are not the separation/deployment times. Instead, they represent the osculating orbit ½ hour after separation from the OSA. H_q and H_Q at the bottom of the table represent perigee and apogee height, respectively.

Epoch Date	23-Nov-2021	21-Dec-2021	13-Feb-2022
Epoch Time	08:33:00	07:17:28	03:06:07
a (km)	199,603.958	200,621.188	200,222.113
e	0.964822	0.965325	0.964944
i (deg)	38.220	38.300	38.293
Ω (deg)	5.117	8.560	4.768
ω (deg)	345.782	353.508	347.471
ν (deg)	136.499	139.130	136.753
H_q (km)	644	578	641
H_Q (km)	385,808	387,908	387,047

BioSentinel's separation orbit is slightly different depending on where it takes place within the launch window. This is explained due to the difference in the position of the launch location and the Moon in inertial space. For instance, for a launch date of 6th June 2022, the LW duration is 112.9 minutes, and the separation orbits are as shown in Table 4.

Table 4. Representative J2000 osculating orbital elements for the BioSentinel separation orbit at LW open and LW close for a 6-Jun-2022 launch date. The osculating elements are J2000 and are both expressed at the Epoch of 6-Jun-2022 23:00:00.0 UTC. BioSentinel deployment times are 6-Jun-2022, 20:38:04 UTC (LW open) and 22:30:57 UTC (LW close) respectively.

Epoch	LW Open	LW Close
a (km)	191,618.898	191,141.148
e	0.964312	0.963778
i (deg)	38.101	28.278
Ω (deg)	23.866	12.280
ω (deg)	26.728	36.635
ν (deg)	146.304	136.981
H_q (km)	460	545
H_Q (km)	370,021	368,981

Once the various BioSentinel trajectories are computed, they are converted to the spice ephemeris format and sent to JPL's multi–Mission Resource Scheduling Services (MRSS) using NASA's Service Preparation Subsystem (SPS) [19]. The duration of these ephemeris files is slightly over a year long. Scheduling of the DSN assets is a negotiation process and is coordinated for the project by the MRSS. Scheduling for BioSentinel was challenging because, besides the Orion capsule, all the CubeSats getting released from the ICPS/OSA also needed DSN support. Table 5 gives sample results for various BioSentinel trajectories computed for different SLS launch dates and with the same deployment assumptions; the time to reach lunar flyby ranges between 5.12 and 5.90 days.

Table 5. Sample LW open circumstances. Time to closest lunar approach (measured from BioSentinel separation Epoch); resulting periselene altitude; and eclipse duration (if no eclipse for that trajectory, then it is shown as n/a). Deployment vector assumptions are the same for all the cases listed.

Launch Date (UTC)	BioS Separation Time (UTC)	Time to Closest Approach (days)	Periselene Altitude (km)	Eclipse Duration (mins)
21-Dec-2021	06:47:28	5.42	1,130	33.3
12-Feb-2022	02:36:58 (13th Feb)	5.32	1,128	23.8
7-May-2022	21:36:58	5.21	1,160	43.0
6-Jun-2022	20:38:04	5.18	579	47.7
3-Aug-2022	21:32:36	5.12	1,153	63.6
2-Oct-2022	22:36:53	5.33	460	40.8
16-Nov-2022	09:49:36	5.25	704	31.2
25-Nov-2022	18:55:00	5.90	436	n/a

In Figure 5 we show the simulated trajectory in the vicinity of the Moon for the August 3rd, 2022, launch date, for LW-open circumstances. BioSentinel (green trajectory) moves from left to right. The resulting eclipse duration is 63.6 minutes.

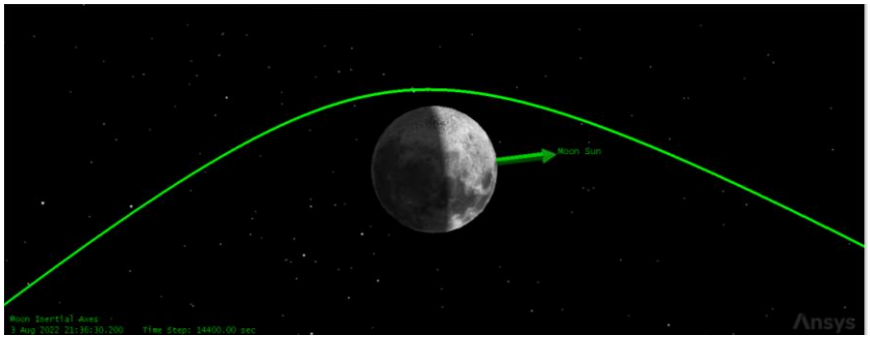

Figure 5. Flyby trajectory for a 3-Aug-2022 launch date (LW open).

In the context of the Earth-Moon circular, restricted three body problem the Hill radius is given by

$$R_{\mathrm{H}} = a_{\mathrm{m}}\left[\frac{M_{\mathrm{m}}}{3(M_{\mathrm{m}} + M_{\mathrm{p}})}\right]^{1/3}$$

where a_m is the Moon's semi-major axis, and M_m and M_p are the Moon's and Earth's masses respectively [20]; it is approximately equal to 6.13×10^4 km, which is the distance from the lunar center to the L_1 and L_2 points. In Fig. 6 we show the evolution of BioSentinel's orbital elements for the specific launch date of February 13th, 2022, from deployment to shortly before lunar flyby. As we get closer to the time of lunar flyby, naturally the perturbation on the elements gets more pronounced. In particular, the semi-major axis increases slightly, but then decreases right after. The eccentricity increasingly approaches unity as we get closer to the flyby time. Interestingly, the inclination eventually becomes retrograde. For context BioSentinel enters the Moon's Hill sphere approximately 4.6 days post-

deployment in this case. The initial separation elements are shown in Table 3. For specificity, in Fig. 7 we show the circumstances for this launch date. BioSentinel's apogee is a little higher than the lunar orbit's radius, and just as it approaches the Moon and proceeds to go beyond $\upsilon = 180^{o}$ in its orbit, lunar gravity pulls it and completely changes its trajectory from an Earth-bound orbit to one on its way to heliocentric space. In this launch date simulation, BioSentinel takes 5.32 days from separation to closest lunar approach, which in this case is 1,128 km from the surface.

We have also found other solutions that (a) undergo a distant lunar encounter and never reach enough energy to reach heliocentric space and (b) lunar impacts. Most of the encountered solutions had favorable periselene altitudes and achieved heliocentric orbit. However, given the variety of potential outcomes (some with serious consequences), we decided to perform systematic Monte Carlo analyses to find patterns in the resulting trajectories.

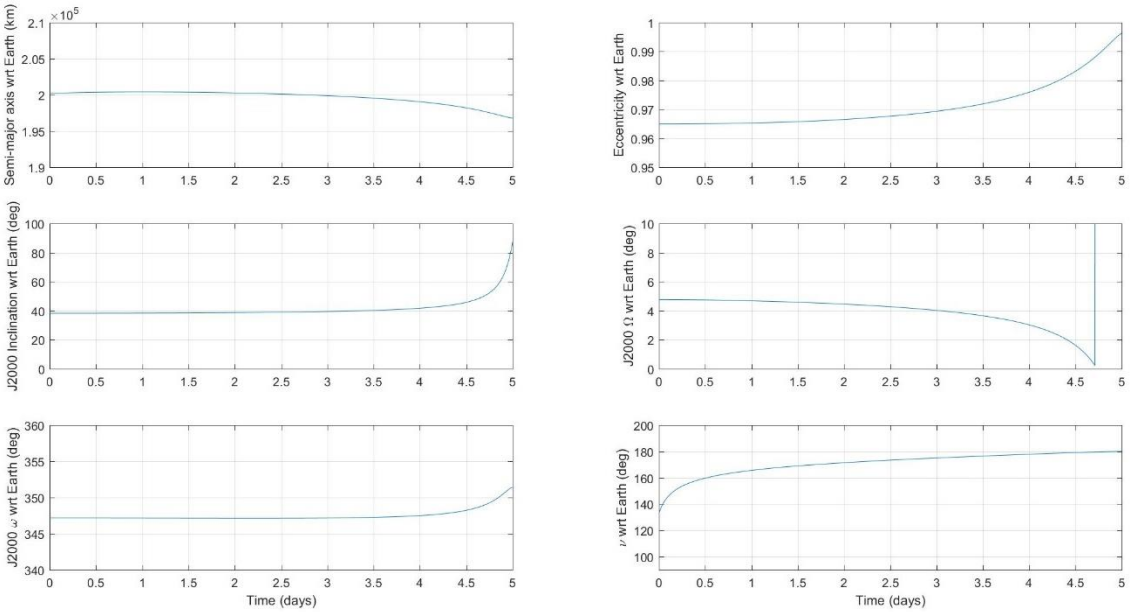

Figure 6. The pre-flyby evolution of BioSentinel's orbital elements (J2000) for the February 13th, 2022, launch date (LW open). Initial conditions are listed in Table 3. BioSentinel enters the Moon's Hill sphere 4.6 days after separation.

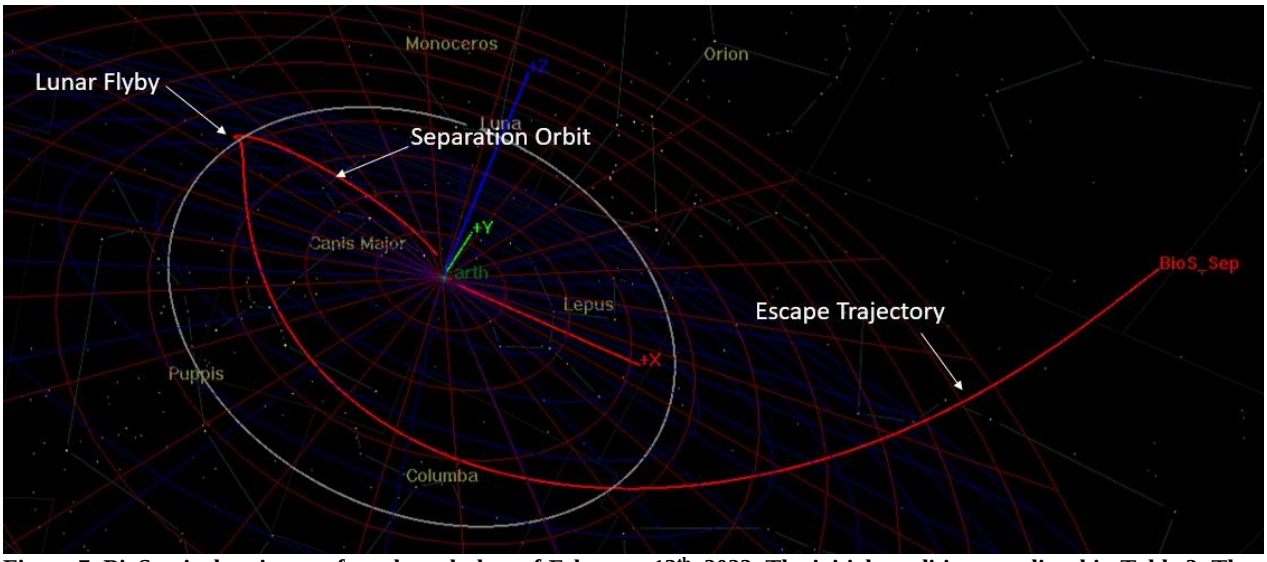

Figure 7. BioSentinel trajectory for a launch date of February 13th, 2022. The initial conditions are listed in Table 3. The propagation time is 27 days. The axes labels represent the Earth Centered Inertial J2000 frame.

IIb. Trajectory Monte Carlo analysis

The main challenge to all the secondary spacecraft aboard the Artemis-I mission was that they were not able to determine their own deployment. After the Orion capsule was deployed, the spacecraft were carried by the ICPS, which was a rotating vehicle that carried a ring where all the spacecraft were stored as depicted in Figure 4.

The rotation rate of the ICPS was 6 deg/s and each satellite was stored at a fixed angle of 56 degrees with respect to the bottom of the cylindrical shape of the ring. The ICPS was shut down prior to the first deployment bus stop and it was not possible to obtain information about the resulting clock angle as a result of the main axis rotation at the time of deployment of each of the satellites. In addition, there was uncertainty associated with the attitude of the ICPS itself and the deployment vector in consequence, as well as regarding the imparted spring force. All those uncertainties must be added to the inherent situation of multiple potential launch periods and hundreds of trajectories within each launch date in the period. For this mission, the results of these analyses were particularly relevant, since a small change in the magnitude and direction of the deployment, a few days earlier than performing a lunar swingby can create a wide range of positions within the B-theta plane, i.e., variations in the altitude of periselene and inclination at the time of the lunar encounter. Some of those wide variations implied the non-trivial risk of a lunar impact. For certain launch dates, the associated planetary ephemeris would yield a high probability of a lunar collision under given assumptions with the deployment vector. To address this scenario, a Monte Carlo analysis was performed for each tentative launch date.

As a result of these simulations, we were able to quantify the probability of lunar impact as well as of achieving the required heliocentric orbit. This outcome was fundamental for the mission to elaborate risk assessments that ultimately led to the decision of implementing a maneuver mode with the onboard propulsion system that was initially only purposed for attitude control. The maneuver mode would provide sufficient ΔV to avert the lunar impact if the burns were performed early enough on the outbound trans-lunar trajectory after deployment. In addition, the results of the Monte Carlo were useful for the Artemis-I mission to discard the probability of collision risk with the Orion capsule and within the secondary spacecraft and the ICPS. The DSN also required the results of these efforts to analyze their potential scheduling conflicts, due to the novel multi-satellite and deep space tracking situation of the Artemis-I mission. Each individual secondary mission was responsible to provide ephemeris per launch date and statistical assessments of their deployments.

The BioSentinel navigation team addresed this situation by running Monte Carlo simulations, taking into account the ICPS rotation, as well as the deployment vector magnitude and the ICPS attitude error. This process had to be replicated several times for the various proposed launch dates, and it was refined and cross-checked with various navigation teams from other Artemis-I secondary missions.

Monte Carlo model description

The Monte Carlo model is a custom software simulation tool built at NASA Ames Research Center for the BioSentinel mission. It consists of a series of scripts that can introduce uncertainties in the initial state of a spacecraft object and later run the propagation in cislunar space. It has also the capability to add maneuvers at custom times, to observe the variability in results in subsequent ΔV is applied after deployment. The software utilizes the epoch and the state vector that is provided by the ICPS team per each launch date. These data include also an estimate of the ICPS atittude at the time of deployment. The main axis of the ICPS is typically oriented between 50 and 60 degrees from ICPS-Sun vector per each case.

This section introduces the mathematical formulas utilized to compute the magnitude and direction of the deployment, including the probability distributions that are introduced to account for uncertainties in the Monte Carlo simulation. The Monte Carlo software utilizes various steps to account for all ucertainties. The tool starts with the calculation of the spring force magnitude, which is converted to deployment ΔV. This is obtained by utilizing the 4-springs curve that was provided by the ICPS team. Figure 8 shows the utilized 4-curve graph to model the imparted deployment ΔV by the spring, which is a function of the spacecraft mass. For BioSentinel, the nominal mass is 12 kg, therefore the nominal spring force is computed at 1.25 m/s. To calculate the equivalent ΔV per case in the Monte Carlo simulation, we introduced a normal distribution with a 3σ of 0.15 kg, and a mean centered in the nominal expected value of the 12 kg BioSentinel wet mass.

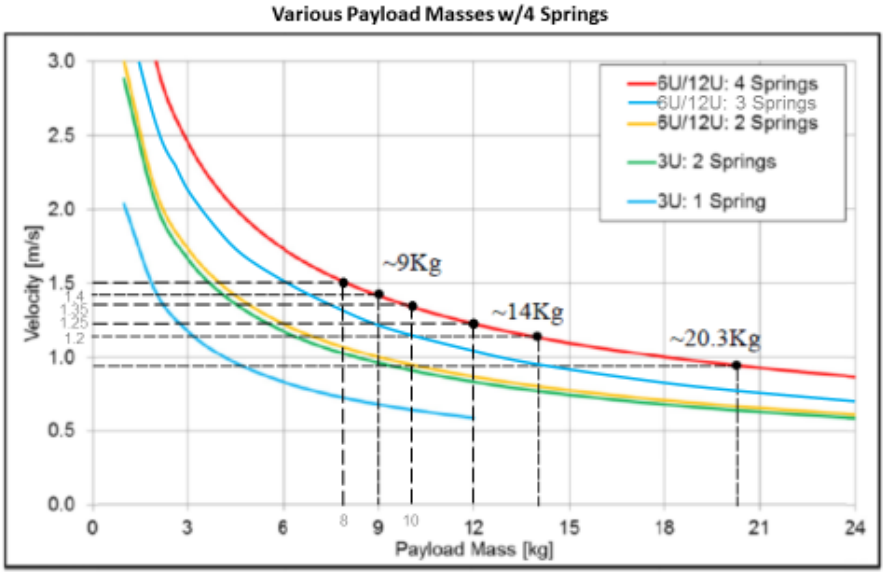

Figure 8: ICPS spring curve. The 4-spring curve was used as a model to compute various magnitudes to account for uncertainties in the spring force of the dispenser.

After the spring ΔV magnitude is computed, the tool computes each component of the deployment vector in the ICPS reference axes, described in the folllowing expressions:

$$Vspring_x = (-1) \cdot deltaV_{spring} \cdot sin(56)$$

$$Vspring_y = deltaV_{spring} \cdot cos(56) \cdot cos(clock_{angle})$$

$$Vspring_z = deltaV_{spring} \cdot cos(56) \cdot sin(clock_{angle})$$

The 56 degrees correspond to the position of the deployment rack as described in the previous section. The clock angle [0,360] is introduced to the Y and Z components in a way that accounts for the random location of the rack at the moment of the deployment. There is no rotation component in the X direction since the rotation occurs around this axis in the reference system that is assumed in the maneuver simulation. This reference system aligns the X component with the main axis of rotation of the ICPS. Therefore, that vector is pointing within by 55 ± 5 deg from the ICPS-Sun vector, each case being slightly different depending on the launch date. Since the ICPS ring is rotating at a constant rate, it is not possible to predict the position of the rack, so we introduce the clock angle to model an arbitrary location at the time of deployment. This rotation only occurs in the Y-Z plane, as we define our reference system. The clock angle is computed using a uniform distribution from 0 to 360 degrees. After that, the software accounts for the tangential component of the velocity given by the rotation of the ICPS ring. Since the X axis is aligned with the main axis, that component is zeroed out. The other two components are computed by using the angular velocity and the radius of the ring according to the following expression:

$$\omega = 6 \text{ deg/s}$$

$$radius = 2.6568 \text{ m}$$

$$Vrotation_{magnitude} = \omega \cdot radius$$

And therefore each component would be the following:

$$Vrotation_y = Vrotation_{magnitude} \cdot cos(clock_{angle})$$

$$Vrotation_z = Vrotation_{magnitude} \cdot sin(clock_{angle})$$

The software also models the uncertainty in the attitude direction of the ICPS. In order to account for that, a rotation about an arbitraty axis is performed. The 3-sigma uncertainty of that rotation is five degrees. The utilized rotation matrix is described in the following equation:

$$R = \begin{matrix} cos(\theta) + x^2 \cdot (1 - cos(\theta)) & x \cdot y \cdot (1 - cos(\theta)) - z \cdot sin(\theta) & x \cdot z \cdot (1 - cos(\theta)) + y \cdot sin(\theta) \\ y \cdot x \cdot (1 - cos(\theta)) + z \cdot sin(\theta) & cos(\theta) + y^2 \cdot (1 - cos(\theta)) & y \cdot z \cdot (1 - cos(\theta)) - x \cdot sin(\theta) \\ z \cdot x \cdot (1 - cos(\theta)) - y \cdot sin(\theta) & z \cdot y \cdot (1 - cos(\theta)) + x \cdot sin(\theta) & cos(\theta) + z^2 \cdot (1 - cos(\theta)) \end{matrix}$$

Several simulations were carried out by using this model per day in the launch window and over three years prior to launch. The simulations were refined each year by adding new assumptions and requirements from the payload office. Eventually, an accurate representation of the attitude of the ICPS per launch date was provided, and was therefore embedded in the model. Most of the time the angle of rotation with respect to the Sun was still within 50-60 degrees. Figure 9 shows an image of the ICPS configuration for a given launch date of 23rd of August.

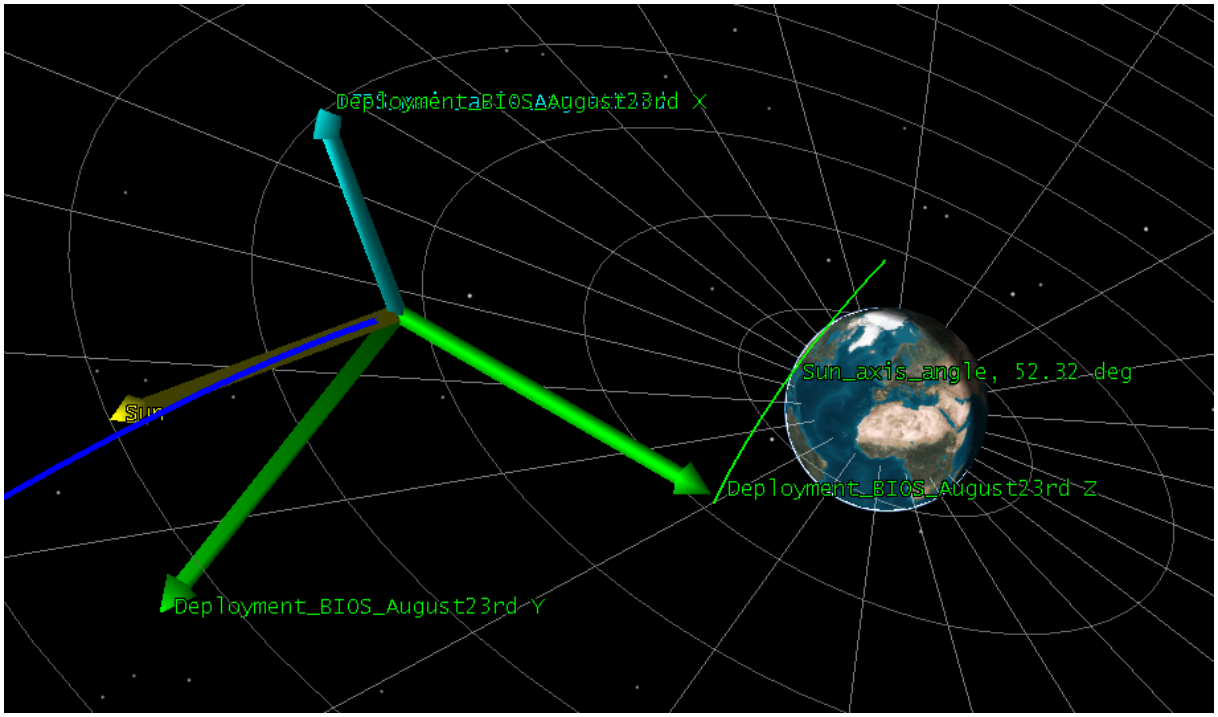

Figure 9: Custom ICPS axis with the x component aligned with the attitude of the ICPS provided by each launch date, in this case on the 23rd of August 2022. The angle with respect to the Sun vector was for all tentative launch dates within 50 and 60 degrees. In this case it was set to 52.32 degrees. The Monte Carlo software utilized a 3-sigma uncertainty of 5 degrees to account for pointing uncertainties.

Using the Propulsion System to avoid lunar impact

BioSentinel was designed as a free-flyer CubeSat, that is, the only change in its orbit was deflection by the lunar flyby into a heliocentric orbit. However, as seen in the Monte Carlo analyses, a non-negligible fraction of trajectories was on a collision course with the Moon, and a maneuver-mode had to be developed in case of such contingency. There was a higher chance of a lunar impact whenever the BioSentinel deployment was oriented in the anti-velocity direction of the flyby trajectory. The idea is that the navigation team will receive and process tracking data from the first three or four passes post-separation to compute a BioSentinel trajectory. The ΔV thruster is located on the body-X face (see Fig. 3). Due to the limitations of BioSentinel's Propulsion system, as well as limitations in the FSW the maneuver needs to be split into several burns, with the following constraints:

- The first thruster burn needs to occur in view of a ground station (however, the following do not need to be in view).
- There shall be a period of two hours between the end of a burn and the start of the next (thermal constraint).
- Each burn shall last a maximum of 31.6 minutes.
- No tracking data available during a maneuver pass.

To raise the periselene altitude, the thruster burns need to be oriented in the velocity direction. In practice, we have found that if a maneuver is needed, it consists between of two and five burns depending on the launch date. After the maneuver is done OD shall determine how effective the burns were at raising periselene altitude. In addition, with post-maneuver tracking data ODTK can solve for the individual burns using the Filter-Smoother combination. Given that the average thrust is 5.3 mN, and BioSentinel's initital wet mass is 11.996 kg, then we can estimate that the maximum ΔV we can obtain per burn is approximately 0.838 m/s.

Monte Carlo Results

The multiple launch periods provided the opportunity to test the results for a wide range of Earth-Moon-Sun geometries. The outcome of this study concluded that depending on the month of the launch period, the resulting trajectories could have a higher or lesser chance of a lunar impact. As an example, launch period 25, which corresponds to the attempted launch date of the 31st of August 2022, provided a high chance of lunar impact, if no maneuvers were performed. Figure 10 shows the results for a simulation with 1000 trajectory cases for the August 29th, 2022 launch date. The statistical analysis showed that 35.1% would result in a lunar impact if no maneuvers were planned.

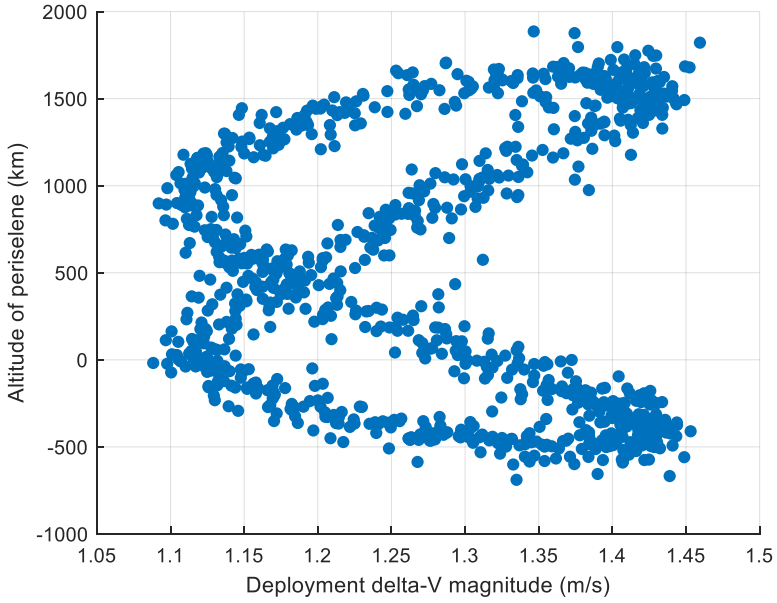

Figure 10: Results distribution of a Monte Carlo simulation with 1000 cases. The altitude of periselene is shown negative which is an indication of how centered the lunar impact in the B-plane is. The deployment ΔV magnitude does not have a significant influence in the altitude of periselene, as cases with higher ΔV are not too distinct from cases with the low end of the spectrum. The main contributing factor is the clock-angle and the ICPS attitude at the time of deployment.

As seen in Figure 10, a significant fraction of the total cases result on a lunar impact, or a low periselene altitude which would also be considered as a major risk for the mission. For this launch date, the mission had to implement a maneuver-mode that could raise the altitude to above the 200 km threshold. The navigation team ran cases that matched the tracking schedule for the various maneuvers, with the goal of having the opportunity to send the command after the third tracking pass, when the orbit determination would be accurate to predict the expected periselene altitude if no maneuvers were performed.

For the August 29th case, several situations were studied, with three, four and five maneuvers. For this case, three maneuvers would have been sufficient to avoid the lunar impact as seen in Figure 11. In this case, the maneuvers would only take place if a threshold altitude of 200 km was activated, since for higher altitudes, the mission would be comfortable to proceed without maneuvering.

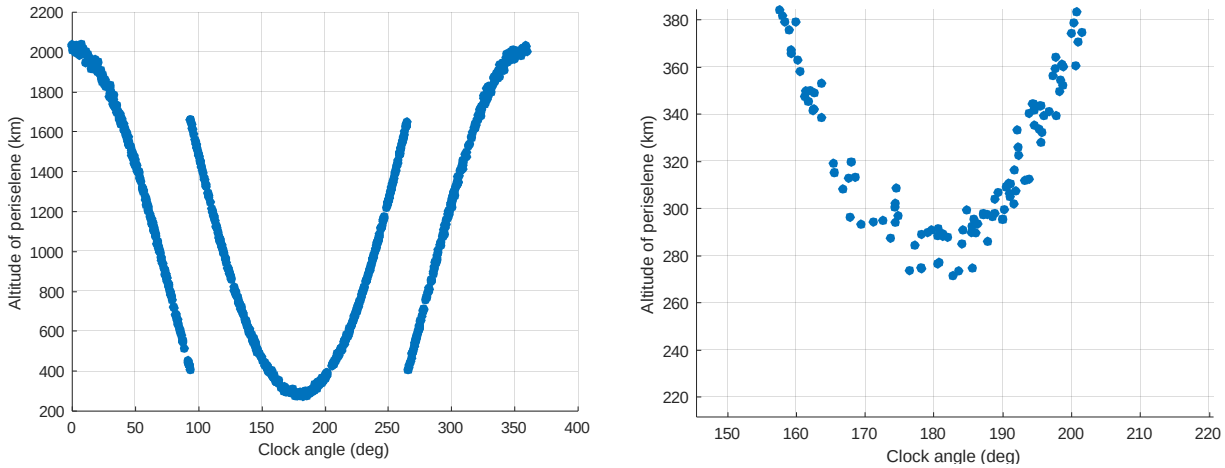

Figure 11: Results of the simulation if three maneuvers are placed. The problematic region around 100-260 degrees for the lock angle is resolved by increasing the altitude of periselene. For that the maneuvers are placed in the positive velocity direction. On the right, a close-up view of the worst-case scenarios.

Another consideration was that for certain launch dates, the achieved C3 energy would not be sufficient to achieve the desired heliocentric space for the mission, due to particular Earth-Moon-Sun geometries. For example, for the August 29th launch date, there was a range of altitudes that would not achieve an Earth-Escape energy. Counterintuitively, those were not the higher altitudes, but within the 750-1250 km range. Lower altitudes than 750 km would get enough energy to achieve positive C3 energy due to their proximity with the Moon, and higher altitudes than 1250 km would also get sufficient energy due to a subsequent Earth flyby. The lesser energy given by the flyby at higher altitudes would mean an Earth return that would be complemented with an Earth flyby that occurs right after. This is a geometry that occurred at only certain launch periods. Figure 12 illustrates this situation for the August 29th launch date. The mission would need to be careful when designing the maneuver strategy, since falling in this range of altitudes would also mean not achieving the mission objectives. Therefore the navigation team designed various maneuver modes to be activated depending on the expected free-flying altitude of periselene achieved after deployment.

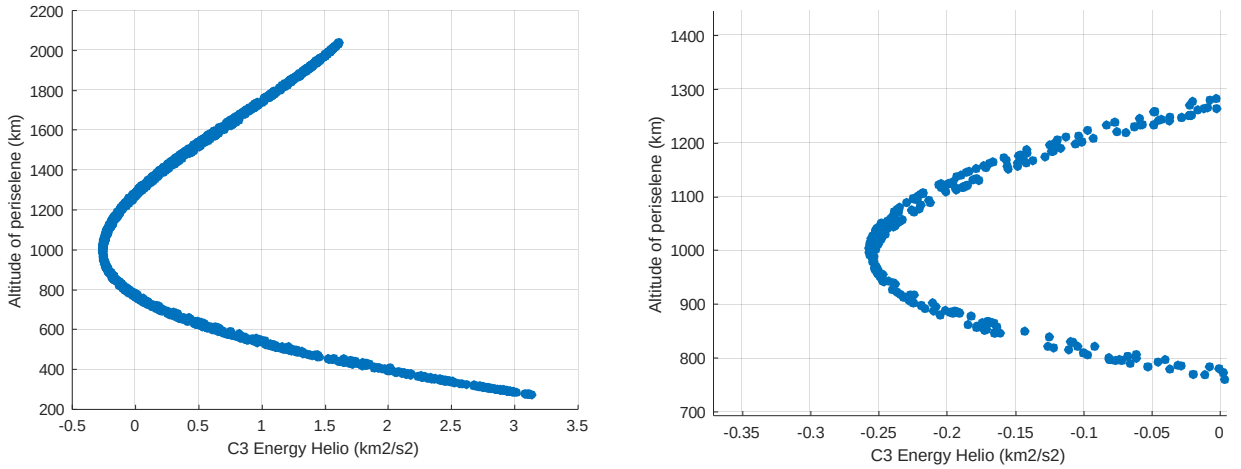

Figure 12. Achieved C3 energy after the lunar flyby for the August 29th launch date. In this case, the relation between altitude and energy is non-linear since higher altitudes benefit from a subsequent Earth-flyby. Altitudes in the 750-1280 km range do not get sufficient energy to leave the Earth-Moon system directly such as with lower altitude cases, and also do not benefit from the Earth flyby as in with higher altitudes.

The situation for the final launch period was more favorable, since the geometry yielded less impact probability. Table 6 shows the trade analysis performed for that launch period.

Table 6: Launch Period 28 Monte Carlo analysis results. For the final launch period, several launch dates were studied, first without any maneuvers and then with various number of maneuvers options that were adapted to the tracking schedule.

Launch date	Number of maneuvers	Maneuver thrust	Minimum flyby altitude achieved in worst case	Maximum flyby altitude	Earth return percentage	Percentage of lunar altitude <300 km
Nov 14th	None	--	Impact	1980.8 km	0% (of the cases that made it)	31.2%
Nov 14th	3 mnvrs	5.3 mN	210.95 km	1983.1 km	9%	0%
Nov 14th	4 mnvrs	5.3 mN	304.5 km	1977.9 km	0%	0%
Nov 16th	None	--	Impact	1987 km	0%	27.8%
Nov 16th	3 mnvrs	5.3 mN	601.11 km	2186.2 km	0 %	0 %
Nov 16th	4 mnvrs	5.3 mN	300.23 km	2186.2 km	0 %	0%
Nov 18th Nov 19th Nov 25th	None	--	Nov 18th : 137 km Nov 19th : 108 km Nov 25th : Impact	--	--	Nov 18th: 17.6 % Nov 19th : 19.8 % Nov 25th : 44.7 %
Nov 18th	3 mnvrs	5.3 mN	301.57 km	2316.3 km	22.7%	0%
Nov 19th	3 mnvrs	5.3 mN	300.79 km	2359.8 km	--	0 %
Nov 25th	3 mnvrs	5.3 mN	Impact	2441.8 km	19.7 %	13.5 %

The results of the Monte Carlo analysis for this launch window showed a non-negligible probability of lunar impact. Therefore the mission added various maneuver modes that would be activated depending on the expected persiselene altitude. The goal was to eliminate the risk of impact while reducing the chances of an Earth return at the same time. Therefore, for some cases there was a need to not overburn in order to create a periselene that would be too high. Figure 13 shows the results of the simulation when 3 maneuvers are placed. As a result, for the conflictive clock angles, the periselene altitude is raised and the risk is mitigated.

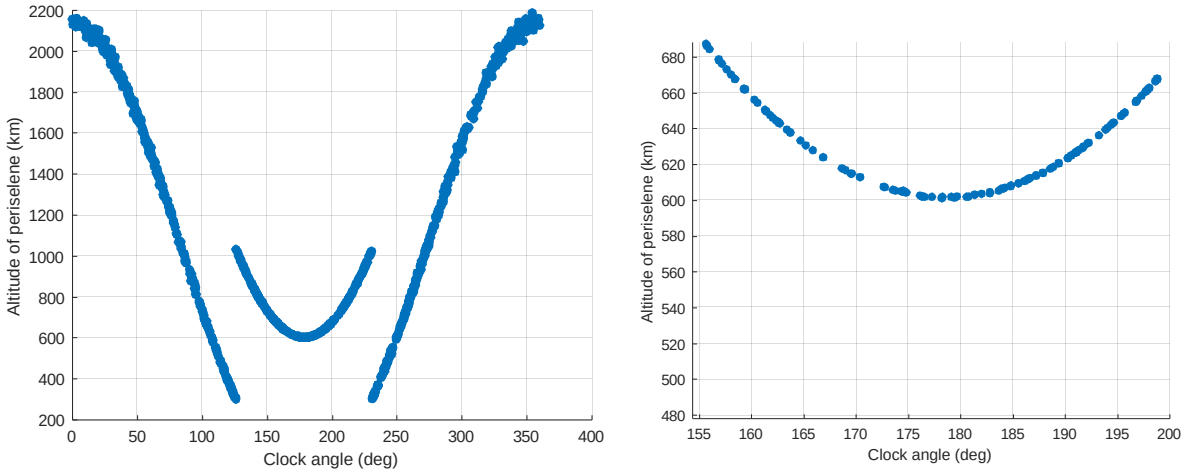

Figure 13. Monte Carlo results when 3 maneuvers are added after deployment according to the tracking schedule. The first maneuver occurs after the third pass and the other two are placed in intervals of two hours. The periselene altitude is always higher than the mission threshold of 200 km.

The resulting cases were all favorable in this case, since three maneuvers did not raise the periselene high enough to cause an Earth return. Figure 14 shows how the Earth altitude range indicates that each trajectory case achieves heliocentric orbit.

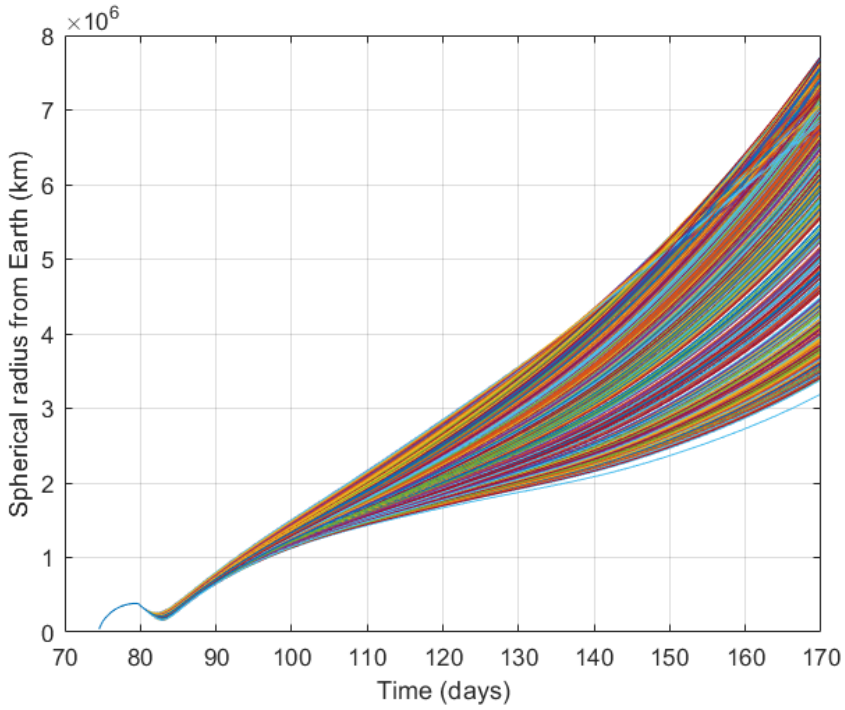

Figure 14. Monte Carlo simulation results for the November 16th launch date with three maneuvers after the third pass. In this case, all the trajectories reach heliocentric orbits since the maneuvers avoid a lunar impact in all cases and they do not raise the periselene altitude too high to create an Earth return scenario.

Another relevant result that was produced for each Monte Carlo simulation was the Sun-Earth-Spacecraft angle. The angle was defined by the Sun-Spacecraft and Sun-Earth vectors. The BioSentinel communications team required an angle below 65 degrees during the first phases of the mission, from deployment to heliocentric orbit. Figure 15 shows that for the November 16th launch date case, all the resulting trajectories comply with this requirement.

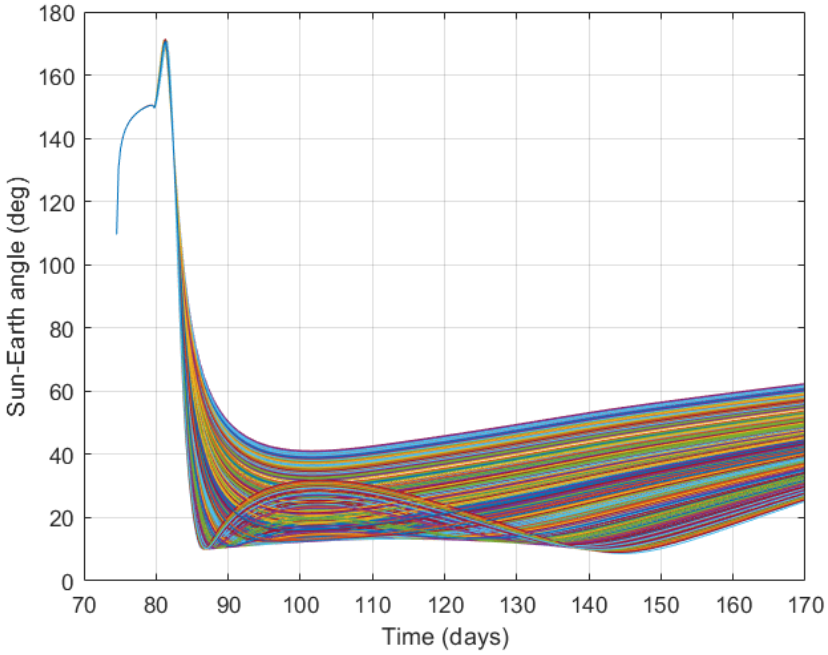

Figure 15. Monte Carlo results that show the angle between the Earth-Spacecraft and the Sun-spacecraft. The mission required an angle below 65 degrees for optimal communication during the first phases of the trajectory. All cases comply with this requirement during that timeframe.

III. Mission Rehearsals

The first mission rehearsals conducted in June 2021 assumed a December 2021 launch date. However, launch dates kept slipping and more simulations and rehearsals took place. Ten rehearsals (Simulations and Operational Readiness Tests, i.e., ORTs) internal to ARC were performed at the Multi-Mission Operations Center (MMOC) with the entire BioSentinel mission operations team, including the navigation team [21]. The navigation team created appropriate propagation and orbit determination scenarios consistent with the given rehearsal launch dates. The former to investigate LW-open and LW-close trajectories (including Earth-Sun angle as observed from BioSentinel), and the latter to investigate the OD characteristics by creating simulated tracking data from DSN and ESA antennas under various assumptions (for instance, evolution of the BioSentinel state vector uncertainty under various conditions). Tested data types were Range, DSN Doppler, DSN TCP and DSN Sequential Ranging. Typically for the navigation team, the rehearsals assumed examination of conditions soon after BioSentinel deployment, but conditions post-lunar flyby and after reaching heliocentric space were also considered. Some rehearsals tested protocols and sequence of events to perform a ΔV maneuver to avoid lunar impact, and for such cases the navigation team provided synthetic lunar-impact trajectories. In parallel, trajectory scenarios were created using the NASA General Mission Analysis Tool (GMAT) as consistency-checks.

In addition, thread-tests were conducted, i.e., software interfaces were tested. The repository for the DSN tracking data is JPL's OscarX system, and access to it was successfully tested. Likewise, once a predicted BioSentinel orbit solution was obtained, the ephemeris file was converted to spice format and uploaded to the DSN Service Preparation Subsystem (SPS) to collaborate in the scheduling process of tracking passes for the Artemis-I mission.

Finally, two ORTs were conducted in conjunction with the DSN and JPL groups in July and August 2022, where the JPL group provided an ICPS orbital parameter message (OPM) containing its orbit and attitude just prior to the CubeSats deploying. In addition, simulated tracking data in the OscarX repository in the TRK 2-34 and TDM formats were also provided. These ORTs were open to all the CubeSat groups, and the BioSentinel navigation team successfully obtained orbit solutions using the OPMs and the provided simulated tracking files.

IIIb. BioSentinel routine orbit determination tools and procedure

The navigation team produced a series of automated scripts to process the tracking data and produce ephemeris. The workflow consisted of processing tracking data, running the orbit determination filter, and delivering outputs to the relevant parties: the mission, the payload office, and the DSN. The process is described in Figure 16. Each pass, and after reviewing the log entry from the previous shift, the first step was to prepare the tracking data. This involved downloading tracking data files from the JPL's OscarX repository to the Biosentinel workstation via the WinSCP program. After the tracking data was available, the next step was to open the Biosentinel orbit determination model and add the new tracking data. Each run the geophysical parameters were also updated to reflect the most current predictions in the force model. Once this is complete, the operator was required to open the orbit determination script and make sure the file path definitions and filter start time epoch were correct. The script ran the Filter and Smoother algorithms and produced a resulting ephemeris file, as well as a series of relevant plots. Then, the operator was required to inspect the data products, which included a measurement data summary, uncertainty plots, and residual ratio plots. After inspection of the data, the operator then added a new entry to the mission log, delivered products to specified locations, and notified interested parties when the ephemerides were uploaded.

OD and data products generation capabilities were included the BioSentinel navigation scripts to perform operational tasks in all phases of operations, including initial orbit determination (IOD), the pre-fly by phase, and post-fly by phase. The orbit determination model included least-square (LS) algorithms, a Kalman filter and a smoother. The LS algorithm is very robust and can be used in case the Filter does not converge. Once a LS solution is obtained it can be used in the next steps which are the Kalman Filter, which sequentially processes observations one at a time, and then the smoother algorithm which runs chronologically in reverse through the data to create a more refined ephemeris.

The primary external delivery from the NAV team was Spice files. During the pre-fly by phase, the navigation team was also responsible for producing Eclipse Duration and Periselene Altitude reports.

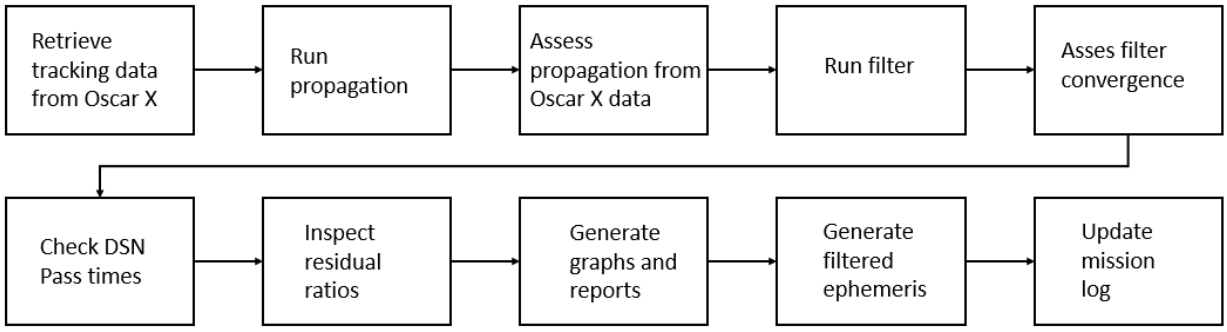

Figure 16. Sequence of events of the Flight Dynamics System. The tracking data is retrieved from the DSN system and then processed to produce a valid ephemeris that is later propagated forward. The resulting file is then uploaded to the SPS portal and to the internal mission repository for ADCS and propulsion system processes.

IV. Navigation flight performance

There were a few SLS block 1 launch attempts from KSC, the first of which occurred 29-Aug-2022. However, the RS-25 engines failed a bleed test. The second and third attempts occurred in September 2022 were aborted due to a LH leak on the 3rd, and hurricane Ian on the 27th. After these aborted launches, the BioSentinel battery was re-charged in October 2022, and another launch attempt occurred 14-Nov-2022. However, the tropical storm Nicole forced a launch scrub.

Finally, SLS block 1 launched on 16-Nov-2022, 06:47:43.92 UTC. The launch time was approximately 44 minutes into the two-hour launch window, which was part of LP 28; see Table 1. BioSentinel was the second CubeSat to separate from the ICPS at 16-Nov-2022, 10:30:42 UTC.

IVa. Pre-Flyby tracking.

For the first orbit determination, the navigation team utilized the initial state vector provided by the ICPS. The tracking data was sparse due to an initial issue encountered by the spacecraft after deployment. The spacecraft ran into a problem with the deposit of the propulsion system that caused it to tumble for several minutes. The mission was able to quickly identify and fix the problem, recovering the planned attitude control of the spacecraft [21]. However, this situation affected the tracking data of the first pass, which was scarce. The procedure was to obtain an OD solution after the first three tracking passes were established in the DSN schedule for our mission. The first pass for which we obtained tracking data was on the 16th of November at 16:25:00 UTC, almost six hours after launch, and the third pass was at 23:20:00 UTC with DSS-43. All passes were scheduled to last for one hour, although the tracking data was sometimes scarcer due to the spacecraft orientation at the time of the pass. After three passes, the navigation team, during the tests and simulations prior to launch, identified that the solution would have enough accuracy to determine the expected altitude of periselene at the time of the lunar flyby. Therefore, after three passes the mission would activate the maneuver mode or not, depending on the probability of encountering a lunar impact.

Due to the partial tracking data pass that occurred after deployment, the descope option in the procedure had to be activated. That required an extra pass to gather enough tracking data to determine the altitude of the lunar flyby. The fourth pass occurred on the 17th of November at 06:05:00 UTC. If activated, the maneuvers would have taken place in the four subsequent tracking passes, according to the Monte Carlo simulation for that launch date, as described in a prior section.

The first four tracking passes from the DSN were TCP data from the antennas DSS-14 and DSS-25 (Goldstone complex); DSS-43 (Canberra); and DSS-55 (Madrid), providing a suitable geographical distribution. After the fourth tracking pass, the LS algorithm utilized in the initial orbit determination process estimated that the altitude of the lunar flyby would be near 400 km. The mission procedure stipulated that altitudes lower than 200 km would be considered for maneuver risk mitigation. Since the altitude was above that established threshold, the maneuver-mode was not activated, and the mission was on its course to a nominal flyby solution. Propagation analysis established that altitude would yield the appropriate energy to achieve the final heliocentric orbit required for the science phase.

The following pre-flyby tracking passes used the Filter and Smoother algorithms described in the software section to obtain BioSentinel ephemeris solutions that best fit the tracking data from the DSN and ESA antennas. The resulting residual ratios[4] of this process are shown in Figure 17. The BioSentinel separation orbit, as well as the estimated deployment ΔV vector is shown in Tables 7 and 8. In addition, with more tracking data a more accurate pre-flyby OD solution predicted a 406 km periselene altitude, with an eclipse start time of 21-Nov-2022, 16:06:56 UTC and a duration of 36.5 minutes. The resulting position uncertainty in each axis (3-sigma) is shown in Figure 18.

[4] Residual ratios are residuals expressed in terms of σ's.

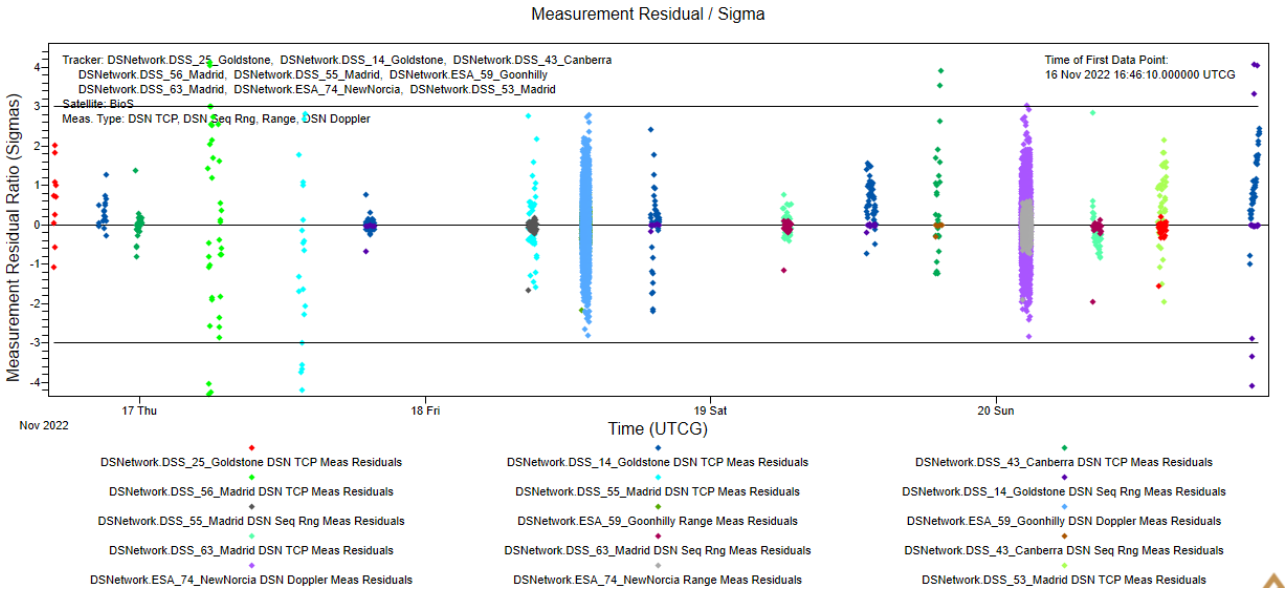

Figure 17. Pre-Lunar Flyby Residual Ratios. Tracking data from DSN and ESA stations were used. Note the diversity in the tracking data type.

Table 7. BioSentinel Osculating Separation Orbital Elements (J2000) at deployment Epoch, from OD results.

Epoch	16-Nov-2023, 10:30:42 UTC
a (km)	195,498.7 km
e	0.964664
i (deg)	30.2527
Ω (deg)	10.9247
ω (deg)	20.4447
υ (deg)	132.984

Table 8. BioSentinel Deployment Vector at deployment Epoch (16-Nov-2023, 10:30:42 UTC), from OD results (Right Ascension and Declination are expressed in the ICRF frame).

Magnitude (m/s)	1.244
Right Ascension (deg)	245.20
Declination (deg)	46.98

In Figure 19 we show the availability of tracking data used for the final pre-flyby OD as a function of time and altitude from Earth, while in Figure 20 we show the BioSentinel trajectory during lunar close approach. Figure 21 shows the BioSentinel Bus voltage during the eclipse, as can be seen the predictions match the observations.

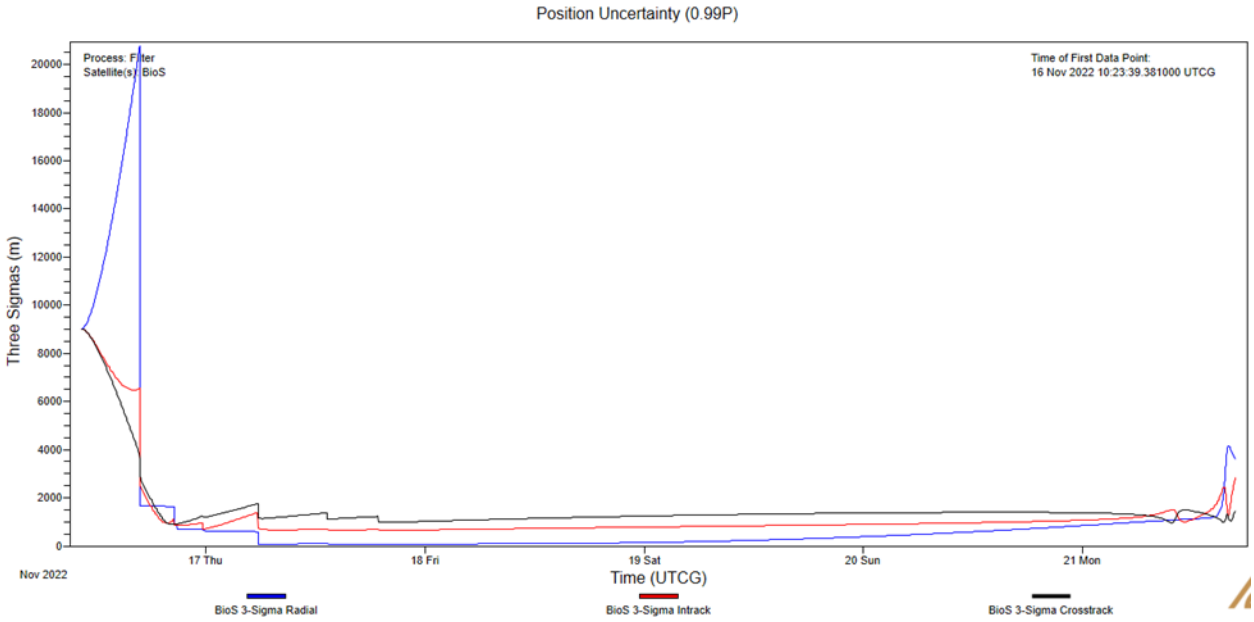

Figure 18. 3-sigma position uncertainty in the RIC frame, from deployment until flyby

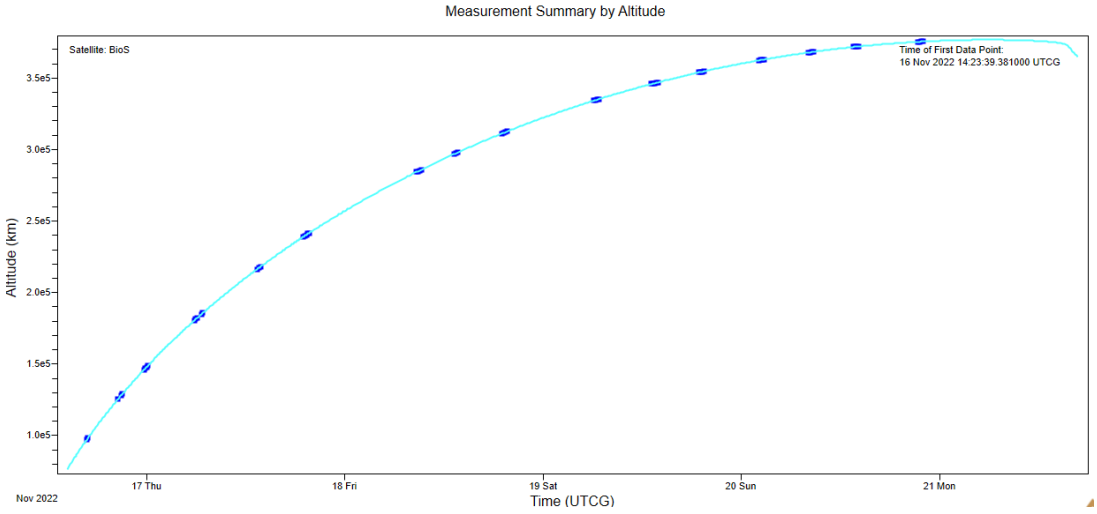

Figure 19. Tracking data passes for BioSentinel pre-flyby OD.

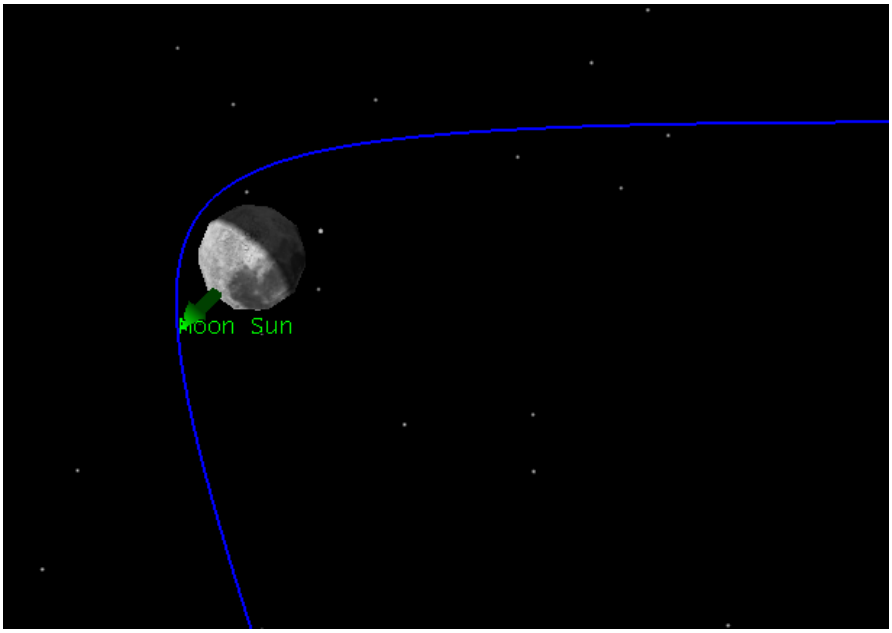

Figure 20. BioSentinel approaches the Moon from below the figure, eventually approaching within 406 km from the lunar surface, a 36.5-minute lunar eclipse follows shortly thereafter.

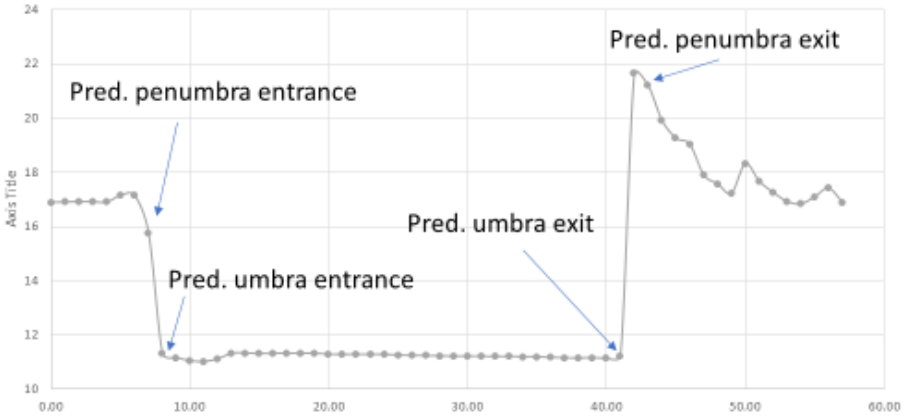

Figure 21. BioSentinel Bus Voltage profile during the eclipse; the eclipse duration was 36.5 minutes. The x-axis shows the minutes elapsed since 21-Nov-2022, 16:00:00 UTC (Voltage data credit: S. Wu, NASA ARC).

IVb. Post-Flyby tracking.

The flyby imposed several challenges, not least of which is the inherent large ΔV imparted by it. The first indication that BioSentinel survived the flyby and resulting eclipse came via signals (and tracking data) from DSS-14 (70 m antenna in Goldstone). Our first post-flyby OD was obtained using a predicted post-flyby trajectory and two DSS-14 passes, as well as single DSS-43 and DSS-63 passes producing mixed tracking data types. The resulting residuals were larger than 3-sigma which is not an acceptable solution. To obtain an acceptable solution we decided to limit the tracking data type to TCP only and to run a LS method which converged, and from there we proceeded as before (Filter, and then Smoother) to obtain an updated trajectory which was converted to the spice format and uploaded to SPS. In addition, to get a valid solution the solar radiation pressure coefficient C_r had to be estimated. Figure 22 shows a residuals ratio plot for the early post-flyby portion of the trajectory.

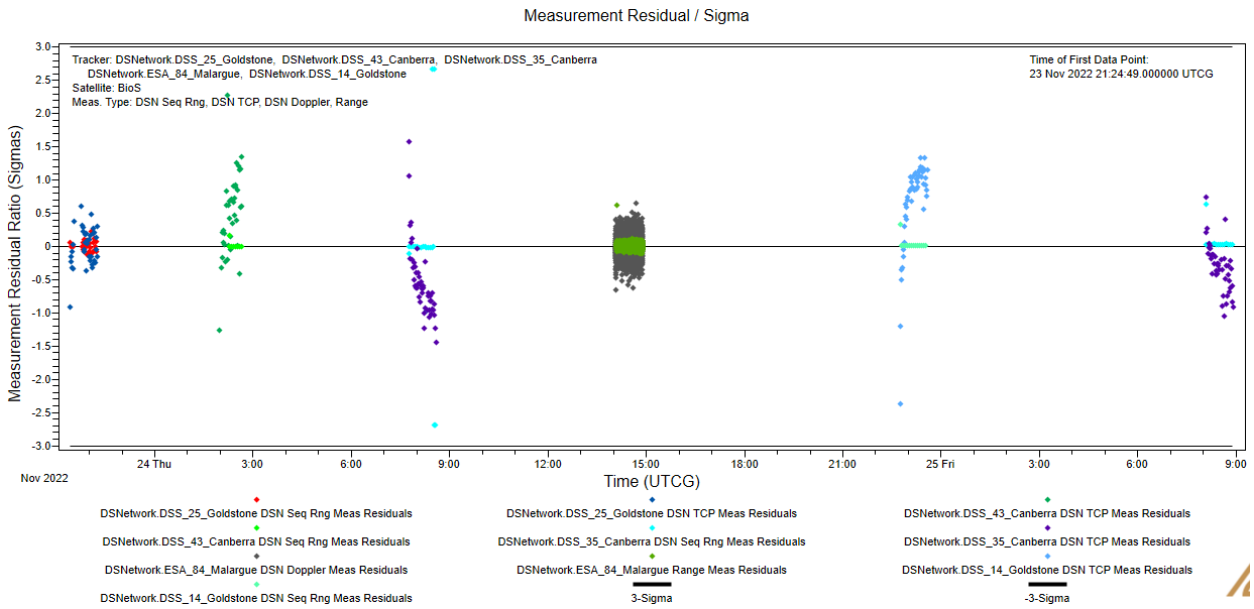

Figure 22. Early post-flyby residual ratios. Several tracking data types are shown, including range, sequential range, Doppler, and TCP.

As the mission proceeded to nominal operations the first momentum-unload maneuvers were performed at the beginning of December 2022. Such maneuvers are performed with the cold-gas propulsion system and unload the accumulated angular momentum due primarily to solar torques. While these maneuvers are generally small, on the order of a few mm/s and smaller, they are incorporated into the BioSentinel force model in ODTK.

In Figure 23 we show the before and after flyby distances to Earth and the Moon, respectively. The minimum distance to the Moon was approximately 2,140 km (406 km from the lunar surface). The minimum post-flyby distance to Earth was approximately 254,060 km, after which point it monotonically increased. The red dashed line at the bottom represents the lunar Hill radius (6.13×10^3 km; BioSentinel spent approximately 1.9 days inside the Moon's Hill sphere).

After leaving the Earth Hill Sphere (approximately 1.5×10^6 km radius), the orbit determination software utilized the Sun as the central body and the Filter had to be reinitialized to account for this change. In Table 9 we show the major sequence of events for the BioSentinel spacecraft beginning with launch from KSC until it left the Earth's Hill sphere.

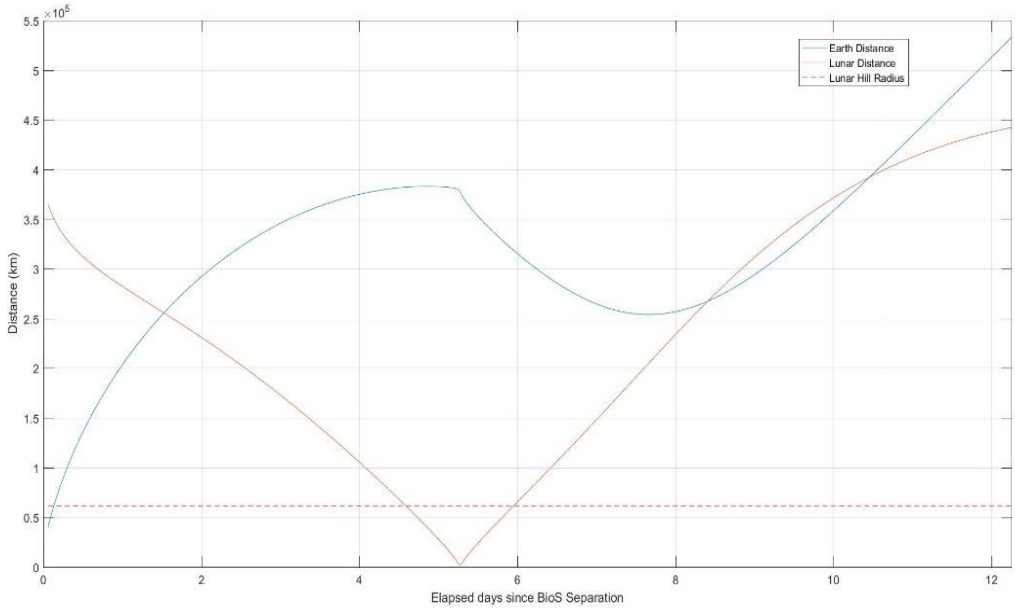

Figure 23. BioSentinel distances to the Earth (blue) and Moon (red) versus time since its deployment. Minimum distance to the lunar surface was 406 km, 5.2 days after deployment.

Table 9. BioSentinel Sequence of Events

Event	Date/Time (UTC)	Time since Deployment (days)	Notes
SLS Launch	16-Nov-2022 06:47:44	-0.155	44 mins. into LW
BioS Deployment	16-Nov-2022 10:30:42	0.0	
BioS Enters Lunar Hill Sphere	20-Nov-2022 23:14:35	4.530	
BioS Closest Lunar Approach	21-Nov-2022 15:40:51	5.215	Periselene alt. = 406 km
Eclipse Starts	21-Nov-2022 16:06:56	5.233	
Eclipse Ends	21-Nov-2022 16:43:23	5.259	36.5 mins. duration
BioS Exits Lunar Hill Sphere	22-Nov-2022 19:47:29	6.387	1.9 days in lunar Hill Sp.
Minimum post-Flyby dist. to Earth	24-Nov-2022 00:54:58	7.600	254,250 km from Earth
BioS Exits Earth's Hill Sphere	12-Dec-2022 10:30:00	26.000	Enters heliocentric space

IVc. Heliocentric tracking.

The lunar flyby provided the necessary energy to achieve an Earth-trailing heliocentric orbit, eventually reaching a heliocentric semi-major axis of 1.018 AU. Routine mission operations continue with the DSN antennas providing typically one pass per week utilized for momentum desaturation maneuvers (when needed) and providing TCP tracking-data for orbit determination. On 9-Jun-2023, BioSentinel reached aphelion at distance 1.038 AU from the Sun, and it will reach perihelion 12-Dec-2023 at a distance 0.998 AU from the Sun. Figure 24 shows sample residual ratios plot of a recent orbit determination solution, on the 25th of October 2023.

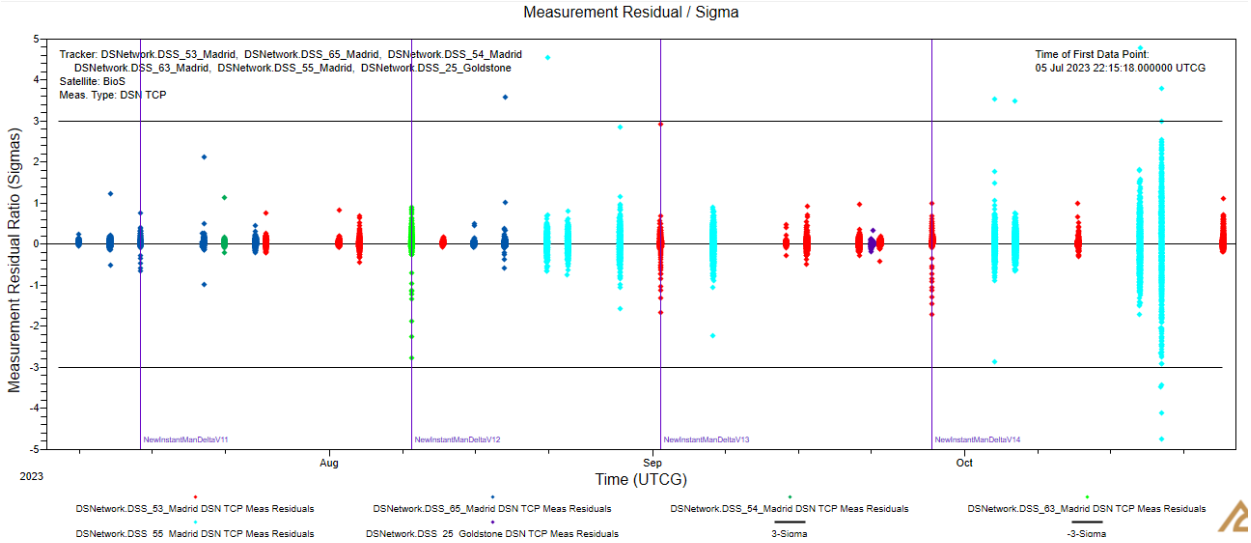

Figure 24. Residual ratios of TCP-type tracking data for BioSentinel in its heliocentric orbit. Most residual rations are within +/- 3σ. Vertical lines represent momentum-dump maneuvers (ΔV's typically on the order of 10^{-3} m/s).

V. Conclusions

BioSentinel is a 6U CubeSat that was successfully launched on November 16th, 2022, aboard the first SLS flight. After separation from the ICPS upper stage, the mission navigation team was able to track and guide the spacecraft from an inbound lunar trajectory, through an energetic lunar flyby, and to a heliocentric orbit, after leaving the Earth sphere of influence. Although unfortunately no biological activity has been detected, the LET spectrometer has been functioning nominally and has been routinely collecting data for active solar events [21].

The preparation prior to flight involved the recurring generation of trajectory ephemeris corresponding to several launch periods. The navigation team also had to construct a suitable flight dynamics system to provide products for the mission, the DSN and the Artemis-I payload office. Several simulations, operation readiness tests and procedures were conducted as part of this effort. In addition, Monte Carlo simulations played an important role due to the inherent nature of the mission.

VI. Acknowledgements

The authors of this paper would like to thank the rest of the ARC BioSentinel team. We would also like to thank following individuals: Laura Plice from NASA Ames Research Center for her contributions during all the phases of the mission; Charles Miyamoto and Gerhard Kruizinga for all the support during the preparations prior to launch and during the campaign navigation phase; and Robert Stough from NASA Marshall SpaceFlight Center for all their insights regarding the ICPS orientation and orbit determination. Finally, thanks also to Ravi Mathur of York Space Systems and John Carrico from Space Exploration Engineering for relevant discussions.

References

[1] NASA's Space Launch System Reference Guide, Version 2.

[2] NASA's Artemis Reference Guide, version 1.0.

[3] Dawn, T.F., J. P. Gutkowski, A. L. Batcha and S. M. Pedrotty, "Trajectory Design Considerations for Exploration Mission 1", 2018. *AIAA SciTech Forum*, 8-12 January 2018 Spaceflight Mechanics Meeting, FL.

[4] Witze, A. "The $93-Billion Plan to Put Astronauts Back on the Moon". *Nature*, Vol. 605, 12 May 2022.

[5] Robinson, K. F., Cox, R., Spearing, S. F. and Hitt, D. "Space Launch System Artemis I Cubesats: SmallSat Vanguards of Exploration, Science and Technology", 2020. *SSC20-S2-05*.

[6] McIntosh, D. M., Baker, J. D. and Matus, J. A., "The NASA Cubesat Missions Flying on Artemis-1", 2020. *SSC20-WKVII-02*.

[7] Diaz-Aguado, M. F., Ghassemieh, S., VanOutryve, C. "Small Class-D Spacecraft Thermal Design, Test and Analysis, PharmaSat Biological Experiment", *Proceedings of the IEEE Aerospace Conference* Vol. 1, 1-9, March 2009.

[8] Tieze, S. M., L. C. Liddell, S. R. Santa Maria, and S. Battacharya. "BioSentinel: A Biological CubeSat for Deep Space Exploration". *Astrobiology*, April 2020.

[9] Padgen, M.R., Liddell, L.C., Bhardwaj, S.R., Gentry, D., Marina, D., Parra, M., Boone, T., Tan, M., Ellingson, L., Rademacher, A., Benton, J., Schooley, A., Mousavi, A., Friedericks, C., Hanel, R.P., Ricco, A.J., Bhattacharya A., and Santa Maria, S.R., "BioSentinel: A Biofluidic Nanosatellite Monitoring Microbial Growth and Activity in Deep Space," *Astrobiology*, February 2021.

[10] Liddell, L.C., Gentry, D.M., Gilbert, R., Marina, D., Massaro Tieze, S., Padgen, M.R., Akiyama, K., Kennan, K., Bhattacharya, S., and Santa Maria, S.R., "BioSentinel: Validating Sensitivity of Yeast Biosensors to Deep Space Relevant Radiation," *Astrobiology*, April 2023.

[11] Lightsey, G., Stevenson, T., Sorgenfrei, M.; "Development and Testing of a 3D-printed Cold Gas Thruster for an Interplanetary CubeSat". Proc. IEEE 106, 379-390, 2018.

[12] Ricco, A. J., Santa Maria, S. R., Hanel, R. P. and Bhattacharya, S. "BioSentinel: A 6U Nanosatellite for Deep Space Biological Science", IEEE Aerospace and System Magazine, Vol. 35, Issue 3, March 2020.

[13] Slobin, S. D. "Deep Space Network 301; Coverage and Geometry". DSN No. 810-005, 301, Rev. M, September 2020.

[14] Wright, J.R. et al. 24-Sep-2020. "Orbit Determination Tool Kit: Theory and Algorithms".

[15] NASA. "EM-1 Space Launch System (SLS) to BioSentinel Interface Control Document". 28 Oct. 2020. SLS-SPIE-ICD-004, Rev. B.

[16] "BioSentinel Deployment for Monte-Carlo Simulation". Dono-Perez, A. 2-Mar-2017. Internal Mission Design Center at ARC memo.

[17] NASA. "SLS Secondary Payloads EM 1 Mission Definition Document". 5 Nov. 2020. SLS-SPIE-DDD-05.

[18] Danby, J. M. A. 1992. "Fundamentals of Celestial Mechanics", 2nd Ed. Willman-Bell.

[19] Bui, B. "Service Preparation Subsystem (SPS) User Interface Portal User Guide". DSN No. 887-000117, Rev. A, December 2018.

[20] Murray, C. D., Dermott, S. F. 1999. "Solar System Dynamics". Cambridge University Press.

[21] Napoli, M., Kong, C., Homan, J., Fusco, J., Nakamura, R., Padgen, M., Wu, S., Shi, P., Benton, J., Heher, D., Stevenson, T., Dono-Perez, A., Alvarellos, J. 2023. "BioSentinel: Mission Summary and Lessons Learned from the First Deep Space Biology Cubesat Mission". SSC23-I-02.

[22] https://www.nasa.gov/specials/artemis-i-press-kit/